

# Defining and Measuring the Performance of Line Protective Relays

Edmund O. Schweitzer, III, Bogdan Kasztenny, Mangapathirao V. Mynam,  
Armando Guzmán, Normann Fischer, and Veselin Skendzic  
*Schweitzer Engineering Laboratories, Inc.*

Published in  
*Locating Faults and Protecting Lines at the  
Speed of Light: Time-Domain Principles Applied*, 2018

Previously presented under the current title at the  
43rd Annual Western Protective Relay Conference, October 2016

Previous revised edition with original title released April 2016

Originally presented at the  
70th Annual Georgia Tech Protective Relaying Conference, April 2016,  
under the title “Defining and Measuring the Performance of Line Protection Relays”

# Defining and Measuring the Performance of Line Protective Relays

Edmund O. Schweitzer, III, Bogdan Kaszteny, Mangapathirao V. Mynam,  
Armando Guzmán, Normann Fischer, and Veselin Skendzic  
*Schweitzer Engineering Laboratories, Inc.*

**Abstract**—This paper focuses on defining and measuring the performance of line protective relays. We review traditional performance measures, such as transient overreach for distance zone 1, and formalize other measures, such as operating time and dependability. We focus on testing ultra-high-speed line protective relays based on incremental quantities and traveling waves. These relays operate primarily in response to transients and therefore require a faithful reproduction of high-frequency components in the test currents and voltages. We provide guidance regarding test signals, propose a number of ways to measure and compare relay performance, discuss the issue of type testing, and review requirements for transient simulation and playback tools for testing ultra-high-speed line protective relays.

## I. INTRODUCTION

Speed, security, dependability, and sensitivity of line protection elements depend on a number of system and fault conditions: source-to-line-impedance ratio (SIR), infeed effect, fault resistance, fault type, and point on wave, to name only a few. How do we define and measure relay performance with so many factors coming into play?

Security is straightforward to define—no operation for all events other than in-zone faults.

Speed is more difficult to quantify, because the minimum, average, and maximum times depend on a number of power system and fault conditions. For example, assuming faults at different points on wave, would lead to different relay operating times. For line faults, what is the realistic statistical distribution of the fault points on wave that we should use while testing line relays for speed?

Dependability and sensitivity are even more ambiguous. For example, what is the dependability of a distance element for resistive faults? We know these elements respond to bolted (metallic) faults, but they would eventually fail to see a fault when the fault resistance becomes too large. Any numerically defined dependability would have to include a complex relationship between the fault resistance, fault location, system impedances, and load flow. As such, it would be application-specific and would not quantify sensitivity in general.

Phasor-based line protection elements are not greatly affected by the traditional challenges associated with quantifying the performance of line protective relays. We expect very high dependability from these elements, with a typical response time in the order of one power system cycle. Phasor-based relays use band-pass filtering to extract fundamental-frequency components from voltages and currents. This internal relay filtering damps transients and

makes the relay relatively immune to high-frequency signal components. As a result, phasor-based relays are relatively forgiving of testing errors as long as the fundamental frequency current and voltage components represent true power system events.

Today, we witness the emergence of new ultra-high-speed (UHS) line protective relays. These relays use incremental-quantities and traveling waves (TWs) to operate in a few milliseconds [1] [2] [3]. To operate at such speeds, these relays use a wide-frequency spectrum in their input currents and voltages. Unlike phasor-based relays, the UHS relays operate in response to changes in their input signals. In order to avoid testing mistakes, we have to apply changes in the test signals, including transients, that represent true power system events. Testing that is tailored to phasor-based relays and inattentive to the high-frequency components in voltages and currents may lead to confusion, wasted time, and false test results.

Because of the speed with which the UHS line protective relays operate, actual scheme tripping times depend more on relay processing times, and TW and optical communications propagation times, and less on the fault and system conditions. On the other hand, the fault and system conditions have a bigger impact on the dependability of the UHS line protection elements. These are new challenges for a protection engineer used to phasor-based protection.

This paper presents both methodology and specific examples of formalized relay performance measures suitable for evaluating new relays and side-by-side comparisons of relay performance.

In Section II, we briefly discuss the purpose, scope, and approaches to various kinds of relay testing: design and manufacturing, certification, and field testing.

In Section III, we review and formalize traditional measures, such as transient overreach, as well as introduce new measures, such as fault current energy.

In Sections IV and V, we focus on defining and measuring the performance of incremental quantity-based and TW-based line protection elements, respectively.

In Section VI, we discuss relay type testing and the difference between fault-induced high-frequency transients and transients applied to test protective relays for electromagnetic interference per the existing IEEE and IEC standards.

In Section VII, we look at transient simulation tools and playback equipment and discuss their adequacy and

requirements for testing UHS relays, especially the TW-based elements.

## II. PURPOSE OF RELAY TESTING

We distinguish three major categories of relay tests [4]:

- Design and manufacturing tests.
- Product certification tests.
- Field tests.

The purpose, scope, and methodology of each of these tests are very different in general, and are dramatically different for UHS relays that are based on incremental quantities and traveling waves.

### A. Design and Manufacturing Tests

These tests include type, functional, validation, and manufacturing tests and are intended to stress the hardware, validate the firmware and associated software, and verify that the equipment has been manufactured as designed. Manufacturers often use custom test equipment and software to run these tests during development and on the production floor.

### B. Certification Tests

Many end users, regional or even national laboratories, require a new protective device to pass a series of tests on a test system of their choice before certifying the protective device for use on their power system. The intent of these tests is to verify that the protective device meets their specified requirements. To be certified, a protective device must operate correctly while being subjected to a series of simulated faults on the test system. These tests are therefore similar to the manufacturer's validation tests but are more specific to the utility's own power system, communications equipment, application philosophy, and so on. The intent of these tests is not only to verify that the protective device will operate correctly on the user's system but also to educate the user on how to set and apply the device correctly.

In addition to these tests, some users subject the device to a custom set of environmental or type tests. Should a protective relay meet all the user requirements, the device is deemed fit for use on the power system.

Certification testing of UHS relays typically requires more expertise and better test equipment and software compared with testing phasor-based relays. The remainder of this paper focuses on certification testing of UHS relays. We expect that many end users may initially turn to manufacturers or specialized laboratories to certify UHS relays, repeating a lesson from the time microprocessor-based relays were introduced to replace electromechanical relays.

### C. Field Tests

These tests are performed in the field on devices installed in their natural environment (panel- or rack-mounted, wiring, test switches, and so on) and interfacing with actual equipment (CTs, PTs, communications links, and so on). The working environment for the field tests is less convenient and controlled compared with bench testing at the manufacturer or in the user's laboratory.

We categorize these field tests as follows:

- Commissioning tests to verify the initial installation, especially the health of the device, wiring, and settings.
- Maintenance tests to check if the installed scheme continues to work properly.
- Troubleshooting tests to find the root cause of problems and prove solutions.

These three categories overlap to a degree and are about a specific installation and its possible failure modes—failure modes primarily caused by human errors. These tests do not confirm that a relay design in general is fit to perform.

This is an important distinction. We can perform field tests of UHS relays using simple test equipment. When field testing, we look for human errors and hardware deterioration, not for the degree of relay performance in general. Also, field testing gives us a chance to obtain and verify some key settings using a line energization test.

## III. LINE PROTECTION PERFORMANCE FUNDAMENTALS

In this section, we discuss how to define, test, document, and visualize line protection performance in general. We focus on underreaching distance elements, overreaching directional elements, and communications-based schemes. Our discussion applies to any relay technology, from electromechanical, to microprocessor phasor-based, to new TW-based line protection.

### A. General Line Protection Performance Measures

We characterize line protection performance using the following performance measures:

- Speed. The time between fault inception and a trip command to the circuit breakers.
- Sensitivity. The ability to respond to low-current line faults as per the assumed fault resistance and system short-circuit level.
- Dependability. The ability to trip line faults under assumed operating and fault conditions with the required speed and sensitivity.
- Security. The ability to restrain for all conditions other than line faults, especially for out-of-zone faults.

Our industry often interprets and formalizes the above general performance measures in a number of ways for the purpose of relay evaluation or comparison. Different approaches may lead to different results, and the differences may become profound for relays that operate at high speeds.

### B. Protection Operating Time

When considering UHS line protection, it makes a difference if we measure the operating time from the fault inception or from the beginning of the disturbance at the relay location. For a 300 km line, the disturbance propagation time is about 1 ms. For a remote fault, we may see a UHS directional element operate in 1.1 ms, if measured from the disturbance at the local terminal, or in 2.1 ms, if measured from the fault inception. Measuring the operating time from the fault inception considers fault effects at the fault location, such as

human safety or property damage. Measuring operating time from the time the disturbance arrived at the terminal is more appropriate when evaluating relay performance. Operating time measured from the time associated with the disturbance arrival at the local terminal removes a variable factor, which we do not have control over—TW propagation time dependent on fault location.

Ultimately, we want to measure the operating time from the fault inception to the moment a dc current starts to flow in the circuit breaker trip coil. From this perspective, interposing relays, if used, shall be included in the operating time tests. When evaluating the operating time for permissive signals, we want to include the relay output actually used with the telecommunications equipment, which is typically a low-energy, high-speed output or a digital interface.

Line protection operating time depends on a number of well-known factors, including these major considerations:

- Fault point on wave, i.e., the instantaneous voltage at the fault location.
- Fault location along the line.
- Line length and system short-circuit level, positive- and zero-sequence for the local terminal and remote terminal (infeed effect).
- Fault resistance or arc-fault voltage.
- Fault type.
- Current and voltage instrument transformer characteristics, especially coupling-capacitor voltage transformers (CCVTs) vs. magnetic potential transformers (PTs).

We know some of these factors for any given application (line length and CCVT type). Several typical values can be considered when evaluating relays in general or for a specific application.

Other factors may change within a known range (system short-circuit level, for example). Proper testing requires us to vary these factors between their realistic limits, while covering all realistic combinations, such as strong remote system and weak local system or vice versa.

We must also consider random factors, such as fault location, type, resistance, and point on wave. Traditionally when testing relays, our industry assumes a uniform probabilistic distribution for these random factors. This means we often assume an equal probability of a fault at the voltage peak or zero crossing, or an equal probability of a single-line-to-ground (SLG) fault and a three-phase (3P) balanced fault, for example. While we can justify a uniform distribution for a fault location, it is not accurate for the other fault characteristics.

Field data tell us that fault type distribution is not uniform at all. Reference [5] mentions that SLG faults are a vast majority in HV systems at about 70 percent, followed by line-to-line (LL) faults at 15 percent, double-line-to-ground (LLG) faults at 10 percent, and 3P faults at 5 percent. Reference [6] provides statistics for extra-high voltage (EHV) systems as follows: SLG at 93 percent, LL at 4 percent, LLG at 2 percent, and 3P at 1 percent. As a result, representative testing for speed should

apply various fault types in proportion that reflect actual fault statistics.

The laws of physics tell us that insulation breakdown is more likely when the electric field is higher. Therefore, line faults are more likely to occur when the voltage is closer to the peak rather than the zero crossing. Yet, because short circuits can have mechanical causes, faults at the zero crossing are still possible. We suggest using points on wave, as depicted in Fig. 1, when testing for speed. For example, each higher voltage level for testing is half the remaining interval between the previous level and the peak. Note that it is important to test both points: when the voltage rises toward the peak and when the voltage falls toward the zero crossing. The relay response times will most likely be different for these two conditions even if the instantaneous voltage at the moment of the fault is the same.

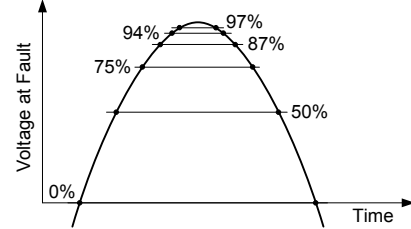


Fig. 1. Suggested fault point-on-wave values.

The point-on-wave consideration applies to the voltage across the insulation that breaks down. For example, when we apply A-phase-to-ground (AG) faults, we should control the point on wave for the AG voltage; when we apply A-phase-to-B-phase (AB) faults, we should control the point on wave for the AB voltage. For LLG and 3P faults, one may consider more points on wave in order to collapse the many voltages involved in these faults when the voltages are at different levels.

The protection operating time is the time elapsed between the fault inception and the trip command. These time markers may become short intervals rather than remain definite points in time. For example, consider the following scenarios:

- Evolving faults such as an AG fault followed by an ABG fault after several milliseconds at the same location. This scenario makes the fault inception a time interval rather than a single point in time.
- Similarly, for an ABG fault, a single-pole-tripping (SPT) relay may trip phase A first, and phases B and C several milliseconds later. This makes the trip instant a time interval rather than a single point in time.

How do we define the operating time in such cases? We can use the maximum time, which is the time interval from the first insulation breakdown to the last per-phase trip output that should assert for any given fault type.

Alternatively, we may use a current-weighted average between the phases that will be tripped for any given fault type. For example:

$$E_{\Phi} = \int_{t_{F\Phi}}^{t_{T\Phi}} (\Delta i_{\Phi})^2 dt, \Phi = A, B, C \quad (1)$$

$$t_{\text{OPERATE}} = \frac{E_A + E_B + E_C}{\frac{E_A}{t_{TA} - t_{FA}} + \frac{E_B}{t_{TB} - t_{FB}} + \frac{E_C}{t_{TC} - t_{FC}}} \quad (2)$$

where:

$\Delta i$  is the incremental (fault minus prefault) phase current,

$t_{tr}$  is the per-phase trip time accounting for a sequential trip,

$t_F$  is the per-phase fault time accounting for an evolving fault.

Line protection operating time always shows a spread based on the factors discussed earlier. Our industry tends to document the minimum, maximum, and average or “typical” operating times, often as a function of fault location and often separately for phase and ground faults. Later in this paper, we discuss other ways of visualizing and comparing the operating time.

### C. Line Protection Sensitivity

Protection sensitivity refers to the ability of detecting low-current in-zone faults under weak system conditions, high fault resistance, or an infeed effect.

Applying fault resistance is a convenient way of testing for sensitivity, but it may lead to skewed results when considering the infeed effect. Arc-fault voltage at the fault location is a more representative fault parameter than fault resistance. Any given arc-fault voltage, such as 60 percent of the prefault voltage, may correspond to very different fault resistances depending on the fault current flowing through the equivalent fault resistance. A uniform arc-fault voltage distribution (such as 0, 10, 20, ..., 90 percent of the prefault voltage) is more realistic than any uniform fault resistance distribution (such as 0, 5, 10, ..., 100  $\Omega$ ). We must also remember that ground and phase faults have very different arc-fault values (low for phase faults and potentially high for ground faults).

We argue that testing to check if the relay responds to faults that depress the fault-point voltage from 100 to 95 percent of prefault value, for example, is a more meaningful test than testing for particular fault resistance in any particular system and for any particular fault location. Specific fault resistance makes sense only after assuming a certain system voltage level and infeed effect. For example, 300  $\Omega$  may be a target for 500 kV systems but not for 138 kV systems. However, a protection system detecting a fault that depresses the voltage at the fault location by 5 percent of the prefault value is considered sensitive in both 500 kV and 138 kV systems.

One particular way of testing for sensitivity can use the voltage level values shown in Fig. 1 and assume a voltage change at the fault point from prefault to 0 percent (metallic fault), 50 percent, 75 percent, etc. of the prefault value. Knowing the desired arc-fault voltage, we calculate the fault resistance for any given fault location and system parameters and apply this resistance in our short-circuit software to generate the test voltages and currents. Consequently, we have a chance to tabulate the results based on the voltage change at the fault location rather than any specific fault resistance.

Knowing the sensitivity in terms of the minimum voltage change at the fault point that can be detected by any particular relay or protection element, an application engineer can confirm if the relay would operate for any particular system, fault location, and fault resistance.

Common expectations regarding line protection sensitivity are as follows [7] [8]:

- Underreaching mho elements respond to metallic faults and have very low sensitivity near the reach point and some sensitivity for close-in faults. Underreaching quadrilateral elements have better sensitivity for all fault locations. The infeed effect greatly impacts sensitivity of both the mho and quadrilateral elements.
- Communications-based schemes (directional comparison or differential) have excellent sensitivity for all in-zone faults and are less dependent on the infeed effect.

We propose to include the aspect of sensitivity in the concept of dependability as explained in the following subsection.

### D. Line Protection Dependability

Our industry does not quantify dependability rigorously. In this paper, we measure dependability as a percentage of total in-zone faults for which a given element operates. A protection element may fail to operate for any given in-zone fault for a number of reasons, such as sensitivity (high fault resistance and/or infeed effect), steady state or transient errors, and natural limitations of the operating principle. For example, a traditional mho distance element may lose dependability for resistive faults close to the reach point. Also, one may consider an operation that is slower than an allowed maximum time as a failure to operate.

We suggest calculating dependability for any arbitrary set of test cases, such as metallic faults, and using the calculated value as a measure of performance.

Fig. 2 plots hypothetical dependability curves for an underreaching distance element set to  $m_0$  (in pu of line length) and an overreaching directional element.

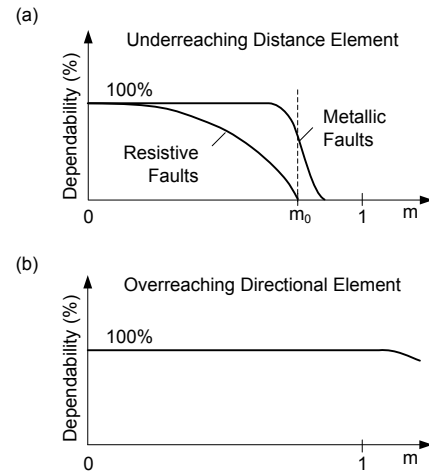


Fig. 2. Dependability curves for underreaching (a) and overreaching (b) elements.

The underreaching element in Fig. 2a responds to fewer and fewer faults as the fault location approaches the reach point,  $m_0$ . It responds to some out-of-zone faults just beyond the reach point. The same element may respond to a much lower percentage of resistive faults. The overreaching element shown in Fig. 2b has a perfect 100 percent dependability for all in-zone cases assumed. It may stop responding to some faults beyond the remote terminal. The transition from operation to no

operation is not typically controlled well for overreaching elements, especially for directional elements as compared with distance elements.

For UHS line protection elements, calculating and plotting their dependability using the convention outlined in Fig. 2 is a good way to evaluate and compare their performance.

### E. Underreaching Elements

Fig. 3 presents an operating time plot and a dependability plot for an underreaching element set to  $m_0$ , as a function of fault location. We plotted two types of designs, superimposed on an ideal underreaching protection element. The ideal element has a uniform operating time up to the intended reach point. At the same time, it retains full (100 percent) dependability up to the intended reach point and stops operating at the intended reach point (0 percent dependability beyond  $m_0$ ). One can argue that such an ideal element cannot be realized in practice, the same way we cannot realize an ideal low-pass filter that makes a step transition between its pass and stop bands.

The practical design marked as A in Fig. 3 is dependability-biased. It retains dependability for faults very close to the intended reach point, while it does not overreach much beyond the intended reach point. This design pays a price for its good accuracy with an increase in the operating time for faults approaching the reach point.

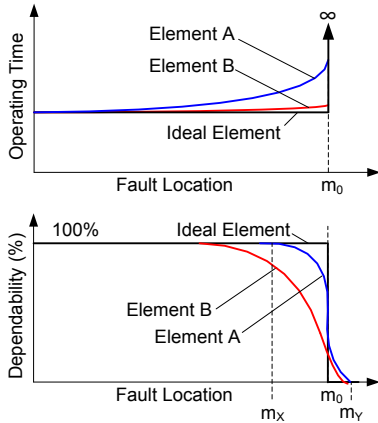


Fig. 3. Sample operating time and dependability curves for an underreaching line protection element.

The practical design marked as B is speed-biased. It retains fast operation up to the intended reach point. This design pays a price for the flat speed curve in dependability near the reach point. Alternatively, this design may retain good dependability up to the reach point, but it would overreach considerably instead.

Phasor-based elements are typically of type A. UHS time-domain elements, such as those described in [1] and [2], are of type B. The UHS underreaching elements are biased for speed, are less dependable, and therefore often require a phasor-based protection element running in parallel to ensure the dependability expected from today's line protective relays. Stated differently, we allow UHS underreaching elements to operate for clear-cut faults, leaving ambiguous cases to conventional protection elements.

Fig. 3 allows us to explain transient overreach (TO), a measure of dynamic accuracy of an underreaching element. For phasor-based underreaching elements, we typically define TO as the difference between the fault location of full dependability ( $m_x$ ) and the fault location of no dependability ( $m_y$ ), as shown in (3):

$$TO = \frac{m_y - m_x}{0.5(m_y + m_x)} \cdot 100\% \quad (3)$$

Typically, we test for TO using metallic faults, and for convenience, we move the element's reach rather than the fault location when testing.

For UHS time-domain elements, definition (3) does not fully apply, because of the large margin between the full- and no-dependability fault locations. For elements that favor speed over dependability, we may define TO as in (4).

$$TO = \frac{m_y - m_0}{m_0} \cdot 100\% \quad (4)$$

Definition (3) focuses on transient accuracy and not on total transient and static accuracy. Definition (4) covers both the transient and static accuracy. Both definitions are valid and applicable to any type of an underreaching element, but they measure different aspects of reach accuracy.

We factor the TO into the margin when setting the element's reach, and consider five percent a very good performance if specified for a wide range of conditions, especially CCVTs and high SIR values.

### F. Overreaching Directional Elements

Characterizing directional overreaching elements for speed, sensitivity, and dependability is similar to characterizing the underreaching elements, except we do not expect them to exhibit much, if any, reach accuracy. Instead, these elements would show faster and less variable operating times and much higher sensitivity and dependability in general.

When characterizing their security, we have to be mindful of their overreaching nature. Directional overcurrent overreaching elements reach so far that it may be difficult for us to label some external faults as forward or reverse based on their perceived location with respect to the relay. The actual direction depends on the incremental current flow in the protected line. As a result, it is convenient to test a pair of directional elements, each located at their respective line terminals, and use a pass/fail condition, taking into account the type of directional comparison scheme that uses the tested elements. For a permissive scheme, the pass condition for security is that the two elements never assert simultaneously in a forward direction for an out-of-zone fault. For a blocking scheme, the pass condition for security is that for each out-of-zone fault, one element asserts forward, the other element asserts reverse, preferably ahead of or simultaneously with the first element.

### G. Communications-Based Schemes

It is best to evaluate communications-based schemes (directional comparison or differential) using closed-loop testing or simultaneous playback to both relays, preferably with the actual communications channel or a realistic replica of the communications channel. This method tests the scheme logic

for communications channel delay, current reversal conditions, or even channel impairment conditions if adequate channel test equipment is available [4].

We can apply the sensitivity and dependability measures discussed earlier to communications-based schemes. When measuring the operating time, we typically record the trip time of the slower of the two relays in the scheme.

#### H. Accuracy of Single-Pole Tripping

In SPT and reclosing applications, trip accuracy refers to tripping correct breaker phases for any given fault type. Specifically, SPT is tripping the correct phase for SLG faults and tripping all three phases for all other fault types.

With respect to SPT, we may encounter the following undesirable relay responses:

- Single-phase trip in the wrong phase. We shall count this scenario as a failure to trip.
- Single-phase trip for a multiphase fault. We shall count this scenario as a failure to trip.
- Three-phase trip for an SLG fault. We shall count this scenario as a form of overtripping.
- Sequential three-phase trip for multiphase faults. We may count this scenario as a slow trip, depending on the degree of the trip output scatter.

We often simulate evolving faults to test accuracy of SPT and consider the following three scenarios:

- Evolving internal fault where one phase is faulted before the other phase(s).
- Internal-to-external fault in which an overvoltage in a healthy phase due to an internal SLG fault creates—within a few milliseconds—a second external SLG fault.
- External-to-internal fault following the same mechanism as the internal-to-external fault.

We typically assume that internal faults begin at a single location (air ionization causes the fault to spread). We also typically assume internal-to-external and external-to-internal faults begin close to one of the line terminals (where the overvoltage is the highest).

We shall test a complete line protection system for SPT accuracy. This shall include the communications channel, because often multibit communications is used between line terminals to improve trip phase selectivity. Note that from the point of view of the remote terminal, a simultaneous internal SLG fault and an external SLG fault look like an LLG fault. The remote terminal cannot resolve the fault type on its own, but it can selectively trip the correct phase based on the multibit communications signal received from the local relay.

#### I. Visualizing and Comparing Line Protection Performance

Let us now look at possible ways of visualizing performance measures for the ease of evaluating and comparing protection performance. Dependability and operating time plots and curves are useful. However, the minimum, average, and maximum operating times do not convey the full picture. A better way—at least when optimizing any given relay design (manufacturer’s perspective) or comparing any two relays

(user’s perspective)—is to look at distribution of the operating time over a range of selected test conditions.

Fig. 4 presents a hypothetical distribution of the operating time for an underreaching element over a range of fault and system conditions, plotted separately for various fault locations. Such a statistical distribution plot allows us to grasp the spread, the best- and worst-case scenarios, as well as the expected mean of the operating time.

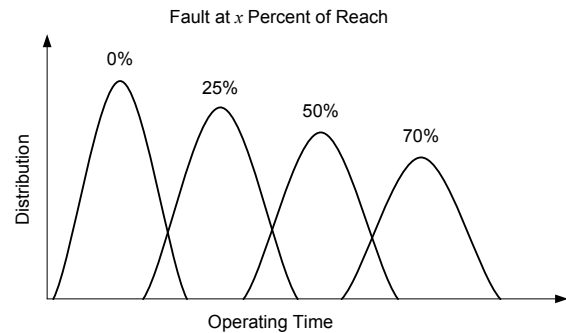


Fig. 4. Operating time distribution for various fault locations.

Using statistical distribution to compare two relays or two designs would be confusing, however. The distributions for the two relays are likely to overlap. This overlap may be misleading because we do not know if one relay is faster than the other for the same or different fault cases. A more insightful way to compare two elements is to calculate the difference in their operating times for each test case separately, and then plot the distribution of that difference as shown in Fig. 5. When plotting the difference, we can truly see how often one element is faster than the other. For example, in Fig. 5, element R is faster in 80 percent of the cases.

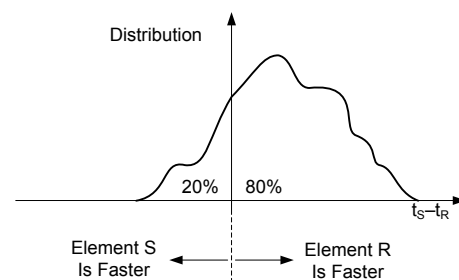


Fig. 5. Distribution of the difference of the operating times between compared protection elements S and R.

Yet another way to visualize and compare the operating time is to use an X-Y scatter plot with the two operating times plotted on the two axes and the dots representing individual test cases, as illustrated in Fig. 6. Using this format, we can show the line of equal speed, as well as the lines of one element being  $n$  times faster or slower than the other.

In addition to tabulating and plotting the operating time, we may consider calculating “fault energy” indices for each test case as per (1). These indices capture the  $i^2t$  energy from the incremental current caused by the fault, integrating from the fault inception until the trip command to the circuit breaker. The faster the trip, the lower the index. The higher the current, the higher the index. This way, we look at the thermal or

electromechanical stress put on the power system from the fault current rather than at the fault duration alone.

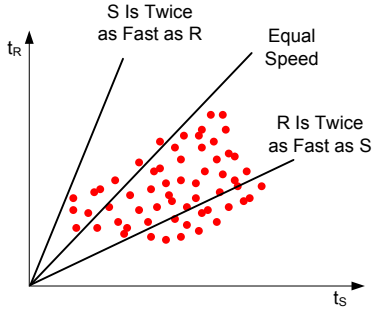


Fig. 6. Comparing protection elements S and R using an X-Y scatter plot.

Using (1), we can average the indices between the faulted phases and compare different fault types. We can plot such normalized indices using the distribution format (Fig. 4), the distribution of the difference between two relays (Fig. 5), or the X-Y scatter plot (Fig. 6).

### J. Importance of Coherent Test Signals

The better the element or relay performance, the more information the relay algorithms and logic extract from the input signals and the more realistic the input signals need to be for proper evaluation and testing. The test signals must contain proper fault-induced components in all frequency bands used by any given relay under test. For phasor-based relays, the frequency band is near the nominal power system frequency. For incremental quantity-based relays, this frequency band is up to several hundreds of hertz. For TW-based relays, this frequency band is in the range of a few hundred kilohertz [1] [2]. One may think of six traditional “loops” when looking at the transmission line (AG, BG, CG, AB, BC, and CA). The applied test signals must be coherent along at least the following dimensions:

- All six loops are consistent with respect to directionality. For a single fault, all six loops shall contain incremental voltages and currents for either a forward or reverse direction.
- All six loops are consistent with respect to the fault type. For example, an AG fault would cause the highest incremental changes in the A phase, while other loops see smaller changes in certain proportions.
- All six loops are consistent with respect to the L/R ratios as driven by the line and system inductances and resistances.
- All six loops are consistent with respect to the  $Z_0/Z_1$  ratios for the line and system.
- The currents and voltages applied to the relay must be consistent with the currents and voltages at the fault location. For example, current and voltage at the fault are of opposite polarities; a fault voltage is lower than a pre-fault voltage, never higher; polarity of the fault voltage is the same as the pre-fault voltage, etc.

These and other characteristics are naturally met when using accurate transient simulation programs or playing back actual fault cases. However, when using test software with heuristic

rules of generating test voltages and currents, one may inadvertently violate the expected relationships between the currents and voltages and cause unexpected test results.

In addition, we need to remember the need to apply legitimate pre-fault voltages and currents before simulating a fault or other switching events. Modern relays measure frequency, develop polarizing signals, or incorporate other checks based on the pre-fault signals before engaging their protection elements. We must make sure to apply a legitimate pre-fault steady-state condition before each test fault.

### K. Importance of Coherent Settings

Meaningful test results require correct settings. Some UHS relays [1] [2] are simple to use and require only a handful of settings. Some settings, such as pickup values or reach, are application specific and users naturally pay careful attention to these settings when testing. Other settings are nameplate settings, such as CT or PT ratios, line impedances, line length associated with a built-in fault locator, or nominal system voltage or frequency. It may seem that these settings are of secondary importance when testing relays. However, they must be accurate because many high-performance relays use these basic application parameters to develop a number of internal coefficients and thresholds. For example, time-domain relays may use line impedances to derive the [R] and [L] matrices required for the calculation of replica currents, or a relay may use the line length to adjust the cut-off frequency of some of the internal low-pass filters. These nameplate settings are readily available and do not require any short-circuit studies, system analysis, or calculations, and they need to be entered correctly.

## IV. DEFINING AND TESTING THE PERFORMANCE OF INCREMENTAL QUANTITY-BASED PROTECTION

This section focuses on the performance of incremental quantity-based line protection elements. This includes the time-domain underreaching directional tripping distance element (TD21) and overreaching directional element (TD32), as well as phasor-based high-speed directional (HS32) and distance (HS21) elements that are based on incremental voltages and currents.

### A. Time-Domain Directional and Distance Elements Based on Incremental Quantities

These elements use incremental quantities—differences between the instantaneous voltages and currents and their one-cycle-old values. As such, the incremental quantities contain only the fault-induced components of voltages and currents. We low-pass filter the incremental quantities with a cut-off frequency of a few hundred hertz so that when deriving the TD32 and TD21 operating equations, we can represent the protected line and the system with equivalent RL circuits.

#### 1) Directional Element

To realize a TD32 element, a microprocessor-based relay calculates the replica current as a voltage drop from the incremental current at the relay location across a unity impedance ( $1 \Omega$ ) RL circuit representing the line and the system. With reference to Fig. 7, the replica current is directly

proportional to the incremental voltage at the relay location [1]. For forward faults, the replica current and incremental voltage are of opposite polarities (Fig. 7a). They are of the same polarity for reverse faults (Fig. 7b).

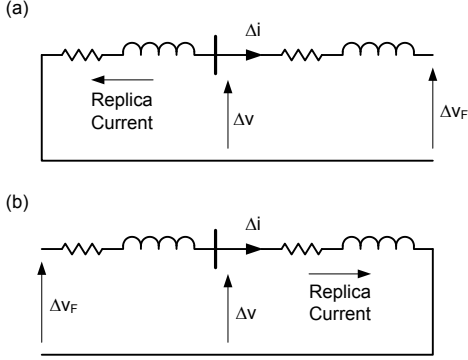


Fig. 7. Operating principle of the TD32 directional element: forward (a) and reverse (b) faults.

Practical implementation of the TD32 element [2] uses all six measurement loops, calculates and integrates an operating torque, and applies adaptive thresholds for optimum sensitivity and speed.

## 2) Distance Element

To realize a TD21 element, a microprocessor-based relay calculates an instantaneous voltage change at the intended reach point using the replica current and the incremental voltage [1]. With reference to Fig. 8, if this calculated voltage is higher than the prefault voltage (highest value possible) at the reach point, the fault must be closer than the set reach,  $m_0$ , and the element is free to operate.

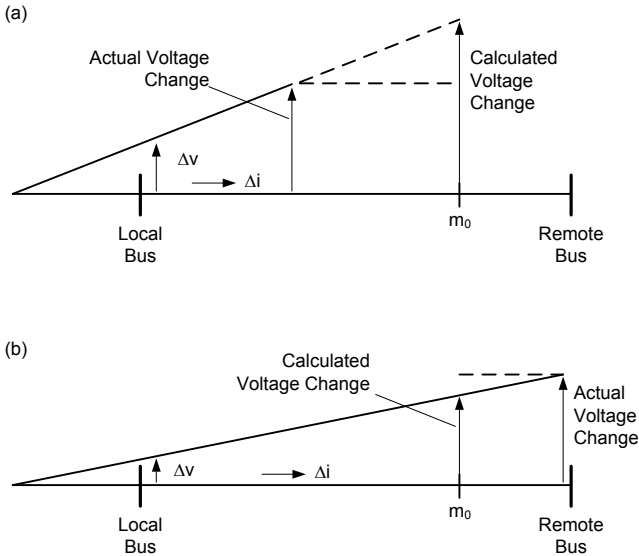


Fig. 8. Operating principle of the TD21 underreaching element: in-zone (a) and out-of-zone (b) faults.

Practical implementation of the TD21 element [2] uses all six measurement loops and applies instantaneous prefault voltage at the reach point as a restraint for optimum sensitivity and speed.

## B. High-Speed Phasor-Based Directional and Distance Elements Based on Incremental Quantities

### 1) Directional Element

A high-speed phasor-based incremental quantity directional element dates back to the 1990s [3]. Its principle of operation is fundamentally the same as the TD32 time-domain directional element in that we use only the pure fault network to derive the operating equations (Fig. 7). The main difference between the time-domain-based element and the phasor-based element is that instead of using low-pass-filtered instantaneous quantities, the phasor-based element uses band-pass-filtered phasor quantities.

To obtain fast operation, the phasor-based element uses half-cycle filters. In addition to determining the direction of the fault, the high-speed directional element (HS32) also determines which phase or phases are involved in the fault. The element calculates an incremental torque quantity using the incremental voltage and incremental replica current half-cycle phasors. The incremental replica current is the incremental current rotated by the conjugate of the positive-sequence line angle. Equation (5) shows the incremental torque calculation for one of the phases.

$$\Delta T_{\phi} = \text{Re}(\Delta V \cdot (\Delta I \cdot e^{-iZ1\text{ANG}})^*) \quad (5)$$

The sign of the torque calculation determines the direction of the fault. A positive torque signifies a forward fault and a negative torque signifies a reverse fault. The HS32 element uses the magnitude of the torque calculation to identify the faulted phases. In practice, the HS32 element is realized by using either a three-phase loop (A, B, and C) or three phase-to-phase loops (AB, BC, and CA). If employing the first of these methods to determine the fault direction and involved phases, and the power system experiences a BG fault, then the logic will declare a forward BG fault if the following conditions are true:

$$(\Delta T_B > \Delta T_A) \ \& \ (\Delta T_B > \Delta T_C) \ \& \ (\Delta T_B > \Delta T_{MIN}) \quad (6)$$

### 2) Distance Elements

Complementing the high-speed phasor-based incremental quantity directional element is the high-speed distance element (HS21). The HS21 element uses the phasor quantities obtained from the band-pass filter in equations for standard distance elements, such as a mho element (7), to calculate the impedance of the fault loop.

$$Z_{HS-\phi} = \frac{\text{Re}(V_{HS-\phi} \cdot V_{HS-\phi} mem^*)}{\text{Re}(I_{HS-\phi} \cdot e^{jZ1\text{ANG}} \cdot V_{HS-\phi} mem^*)} \quad (7)$$

Since speed is the primary requirement for the distance element, the band-pass filter must introduce a small delay. One particular design uses a half-cycle Fourier filter. Using this design, corresponding directional and fault identification elements enable the HS21 element.

## C. General Testing Considerations

These elements require an incremental change in both voltage and current. Therefore, traditional testing methods, where voltage or current is held constant and the other is slowly varied, do not work.

Furthermore, the incremental change in voltage and current needs to occur within the time period expected by the element. The magnitude of the incremental change during this time period needs to be large enough given the respective minimum threshold requirements. For example, assume that the directional element described by (5) has a one-cycle window and that the required minimal incremental torque for the HS32 element is 50 VA secondary ( $\Delta T_{\text{MIN}}$  (6)). If so, the applied test quantities need to generate an incremental torque greater than 50 VA in a time period of 1 cycle in the phase of interest.

When testing any protection element, we need to evaluate the four dimensions of performance as discussed in Section III: security, dependability, speed, and sensitivity.

### 1) Security

These elements respond to rapid incremental changes (step changes) in voltage and current. Switching transients on a power system, such as line reactor energization and de-energization or bypassing of an in-line series capacitor, generates transients similar to those of a genuine fault. Therefore, the incremental quantity-based protection elements must discriminate between switching transients and fault-induced transients. Switching events are even more important if the switching occurs within the zone of protection (reactor or capacitor switching). These switching conditions not only create transients with a similar signature as fault conditions but they also generate off-nominal frequencies that are only slightly attenuated by the band-pass or low-pass filters. As a result, the accuracy of distance elements (TD21 and HS21) may be compromised, depending on the magnitude of the off-nominal frequency components. Therefore, a suite of tests needs to be generated that simulates these switching conditions and external fault conditions. Testing the incremental quantity-based elements using fault quantities that contain only nominal frequency components generally does not sufficiently challenge the security of these elements.

CCVT transients are known to challenge the security of distance elements, especially for systems that have a high SIR. Note that a high SIR does not imply a weak power system, especially if the protected line is short. Select the test condition so that you have a high SIR and develop enough incremental current to enable the high-speed elements. One method uses a short transmission line and adjusts the source impedance to get the desired SIR voltage, while still developing sufficient incremental current to keep the high-speed elements engaged.

### 2) Dependability

Often, for these elements to be enabled (armed), the power system must be in a quiescent condition for a certain time period before applying the fault or transient condition. This is so that the elements have a stable reference quantity from which to calculate their incremental quantities. Ensure the pre-fault time interval is long enough to avoid failures to trip when testing for dependability.

The main criteria that challenge the dependability of the incremental quantity-based elements is whether the fault generates high enough incremental voltage and current quantities given the minimum pickup thresholds (factory or

user settings). To evaluate dependability, we have to determine which factors impact the incremental change in voltage and current for an in-zone fault. The following factors determine the incremental voltage for a fault condition:

- Distance to the fault.
- Prefault voltage (point on wave).
- SIR of the systems as seen from both terminals.
- Fault resistance or arc-fault voltage (see Section III).

The total impedance between the source and the fault point determines the incremental current, irrespective of the SIR. For the incremental current quantity derived from the instantaneous quantities (low-pass filtered), the pre-fault voltage (point on wave) at the fault point determines the incremental current and the rate of change of the incremental current.

Fig. 9 shows an example of a dependability curve for a sample TD21 element [2] tested for a 161 km, 500 kV line with an SIR of 1.4 at both terminals. As expected, the element responds to fewer faults as the fault location approaches the set reach.

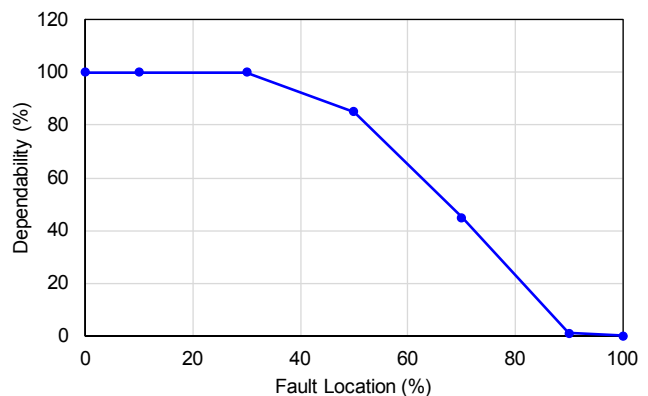


Fig. 9. Sample dependability plot for a TD21 element.

As mentioned previously, the high-speed elements are only enabled if the power system is in a quiescent condition before the fault occurs. Therefore, these elements cannot reliably detect faults immediately following line energization or reclosing.

### 3) Speed

The speed of the incremental quantity-based elements is primarily determined by how rapidly the required incremental quantities develop. This is primarily a function of the impedance between the source and the fault point, and the voltage change at the fault point. The latter depends on the pre-fault voltage at the fault point (point on wave) and the fault resistance (arc-fault voltage).

What is interesting to note for the instantaneous incremental quantities element is not only the pre-fault magnitude of the fault voltage but also whether the pre-fault voltage was increasing or decreasing in magnitude at the moment of fault inception. In general, for the same initial pre-fault voltage, if the pre-fault voltage was increasing in magnitude at the time of the fault, the rate at which the incremental quantities develop is more rapid than if the pre-fault voltage at the time of the fault was

decreasing (see Fig. 1). For the phasor-derived incremental quantities, the prefault voltage does not play as dominant a role as in the instantaneously derived incremental quantities. This is due to the effect of the band-pass filtering. The speed of operation of these elements within the protection zone is relatively constant, irrespective of the location of the fault. However, what does change with fault location is the dependability of the element.

As the fault moves closer to the reach point, the dependability of the element decreases (see Fig. 9). This is because the required incremental quantities do not develop rapidly enough and the operating margin is getting smaller. This effect becomes more pronounced when the line includes series compensation or when lines with series compensation share a common bus with the protected line.

Fig. 10 presents a plot of the TD21 operating time as a function of fault location and the SIR for faults on a 161 km, 500 kV line.

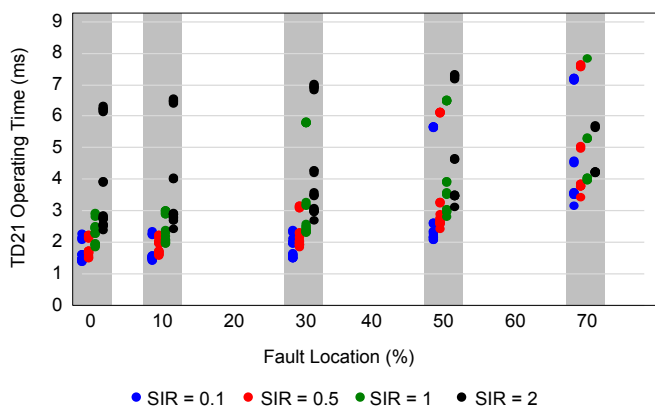


Fig. 10. Sample operating time plot for a TD21 element.

Fig. 11 compares a sample phasor-based underreaching element (PH21) with a TD21 element using 1330 fault cases.

To provide protection for the entire transmission line, the high-speed underreaching distance elements are complemented by the high-speed directional element typically using a permissive scheme, such as a permissive overreaching transfer trip (POTT) scheme. Often, the channel delay may be significant by comparison with the response time of the directional elements, especially the TD32. In the POTT logic, the received signal from the remote terminal must coincide with the forward indication from the local terminal in order to execute a high-speed directional comparison trip. If the channel delay is too large, these two signals may fail to coincide and the directional comparison scheme may fail to operate. Practical POTT designs deal with this issue and they should be tested under realistic channel latency conditions. A further issue with the high-speed directional elements, especially if the protected zone contains series compensation, is that the directional elements may not remain asserted continuously during the fault due to the influence of the off-nominal frequency components. Therefore, in order to verify the correct operation of the POTT scheme, we must verify that the received signals coincide with the local directional elements given the actual channel latency.

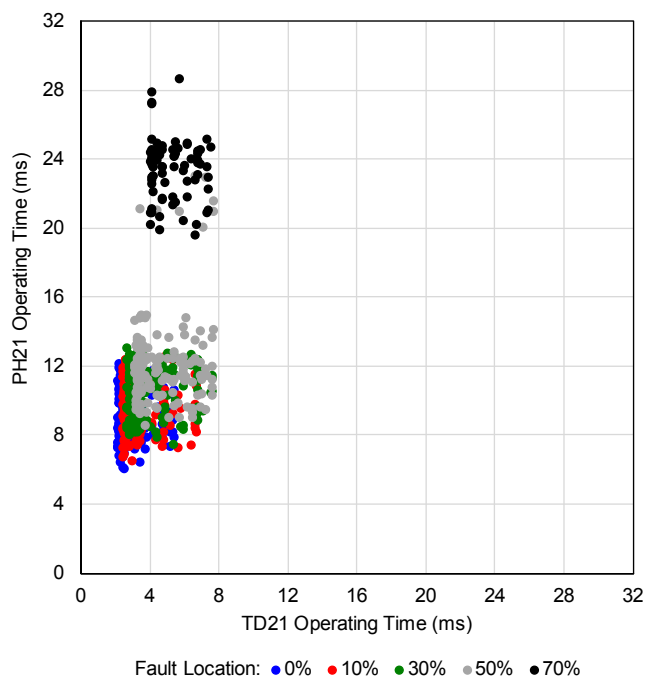


Fig. 11. Speed comparison of a sample phasor-based PH21 element with the TD21 element.

#### 4) Sensitivity

The high-speed elements require an incremental change in voltage and current within a fixed time interval. If the incremental quantities do not develop within the required time, the elements will not respond. We cannot easily determine the maximum fault resistance as it is primarily a function of the voltage depression caused by the fault condition. The voltage depression magnitude is a function of the fault resistance and the impedances from the fault to the two sources. Therefore, the sensitivity of the high-speed elements is not only dependent on the resistance of the fault but also the distance to the fault and the strength of the respective sources (see Section III for a discussion about using the voltage change at the fault location as a measure of sensitivity).

From the above, we can see that in order to test these elements and obtain credible results, we need to use realistic prefault and fault signals. An electromagnetic transient program (EMTP) simulation [9] can provide these test signals. Since the frequencies of interest for these elements are typically below 1 kHz, a sampling frequency of 10–20 kHz is adequate for creating these test cases. Most modern test equipment is capable of replaying transient files, such as COMTRADE, at these sampling frequencies.

Fig. 12 presents TD21 operating times as a function of fault resistance and location for a 161 km, 500 kV line. As expected, the element is faster for close-in and metallic faults, and it operates for close-in faults with fault resistance.

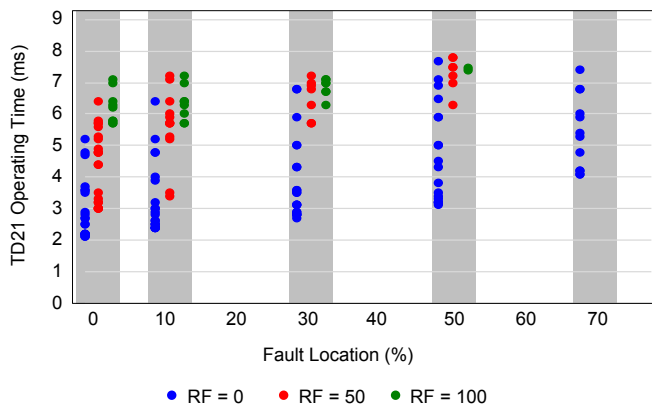


Fig. 12. TD21 operating time as a function of fault resistance for sample system conditions.

## V. DEFINING AND TESTING THE PERFORMANCE OF TW LINE CURRENT DIFFERENTIAL PROTECTION

This section focuses on the performance of the TW-based line current differential element, TW87.

### A. TW87 Principle of Operation

The TW87 element compares time-aligned current TWs at both ends of the protected line. For an external fault, a TW that entered one terminal with a given polarity leaves the other terminal with the opposite polarity exactly after the known line TW propagation time [1]. To realize a TW87 element, a microprocessor-based relay extracts current TWs from the local and remote currents, identifies the first TWs in local and remote currents, searches for exiting TWs a known time after the first TWs, and calculates the operating and restraining signals from the first and exiting TWs.

Practical implementation of the TW87 element [2] uses real-time fault location information and other security conditions in addition to the pickup and slope settings customary in any differential protection logic.

### B. Test Equipment Requirements for Testing TW Protection Elements

Protection elements using TWs consume data recorded at a high sampling rate (megahertz) with signal bandwidth in the order of hundreds of kilohertz. Some of these elements, for example TW87 and TW fault location, in addition to wave magnitudes and polarities, require a common time reference to evaluate the waves captured at the two line terminals.

Fig. 13 plots a sample phase current fault transient while Fig. 14 shows an enlargement of the phase current shown in Fig. 13 along with the extracted high-frequency signal (blue) using the differentiator-smoother, described in [10]. The phase current in Fig. 14 is a steep step with the magnitude of several secondary amperes. Therefore, test equipment used to test TWs must be able to generate steps with a rise time of a few microseconds and magnitudes of several secondary amperes. For more accurate testing, such as when certifying the relay, subsequent steps representing reflections of TWs that traveled some distance should represent the effect of attenuation and dispersion. Some TW protection elements could also require

the presence of a system frequency signal for both pre-fault and fault components along with the step. The pre-fault signals may be required in order to establish if the algorithms should run. The fault components may be required for supervision of the TW protection elements.

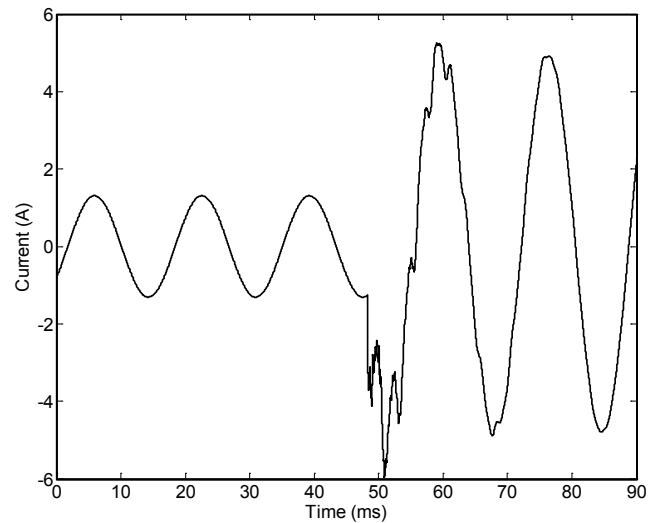


Fig. 13. Phase current during a phase-to-ground fault.

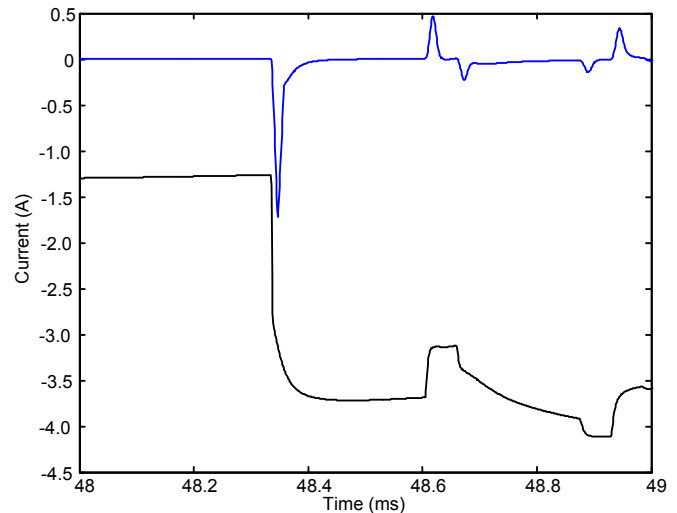


Fig. 14. Differentiator-smoother extracts the high-frequency signal (blue) from the phase current (black).

Today's protective relay test equipment is not designed to provide a fast rise time to emulate steep steps in the order of microseconds. For example, one popular test set is capable of providing a 130  $\mu$ s rise time on its output for a step input. Although, this performance is adequate for testing phasor-based elements and elements using incremental quantities, it is not adequate for testing TW-based elements.

Section VII discusses relay test set applications for testing with both step changes and lower frequency voltages and currents. An alternative way of testing protection elements is to use an EMTP to model power system events, generate test signals, and play back the signals to the relay—also discussed in Section VII.

When playing back test signals, one needs to make sure the amplifiers have adequate bandwidth to represent TW events. In order to simplify this kind of testing, some UHS line protective relays are equipped with built-in playback functionality. This feature allows uploading the transient signals to the relay memory and triggering the relay to use these data to substitute the voltage and current samples from the analog-to-digital converters.

### C. Evaluating the Performance of the TW87 Element

The performance of the TW87 element shall be evaluated using the same key measures discussed earlier: sensitivity, dependability, security, and speed.

#### 1) Sensitivity

A TW is a sharp change from one quasi-steady level to a different quasi-steady level. For a resistive fault, the current magnitude of the change launched at the fault location is dependent on the following factors as represented by (8).

- Voltage magnitude at the fault location for the faulted loop ( $V_{SYS}$ )
- Point-on-wave angle (POW)
- Fault resistance ( $R_F$ )
- Line characteristic impedance ( $Z_C$ )

$$I_{STEP} = \frac{\sqrt{2} \cdot V_{SYS} \cdot \sin(POW)}{Z_C + 2 \cdot R_F} \quad (8)$$

The current TW magnitude measured by the relay is further dependent on the termination characteristic impedance ( $Z_T$ ) and the current transformer ratio (CTR) as shown in (9).

$$I_{RELAY} = \frac{I_{STEP}}{CTR} \cdot \left(1 + \frac{Z_C - Z_T}{Z_C + Z_T}\right) \quad (9)$$

For an SLG metallic fault at the voltage peak on a 500 kV system, the measured current is 3.0 A secondary ( $Z_C = 300$ ,  $Z_T = 150$ ,  $CTR = 3000/5$ ). For the same fault with 100  $\Omega$  of primary fault resistance, the relay would measure 1.8 A secondary. Relays equipped with TW functionality are capable of providing meaningful measurements as low as 50 mA secondary (one percent of nominal current).

Following equations (8) and (9) and knowing the operating logic and applied settings of any given TW87 element, we can analyze the sensitivity of the TW87 protection element. For any given voltage level, CTR, line characteristic, or line terminal termination impedance, we can calculate the POW for which the element will operate for any given fault resistance. We can also calculate the maximum fault resistance for any assumed POW.

Fig. 15 presents a sample plot for a 500 kV line, with the characteristic impedance of 300  $\Omega$ , and termination impedances of 150  $\Omega$  at each line terminal, 3000/5 CTR, and the minimum pickup setting of 300  $A_{rms}$  primary or 0.5  $A_{rms}$  secondary.

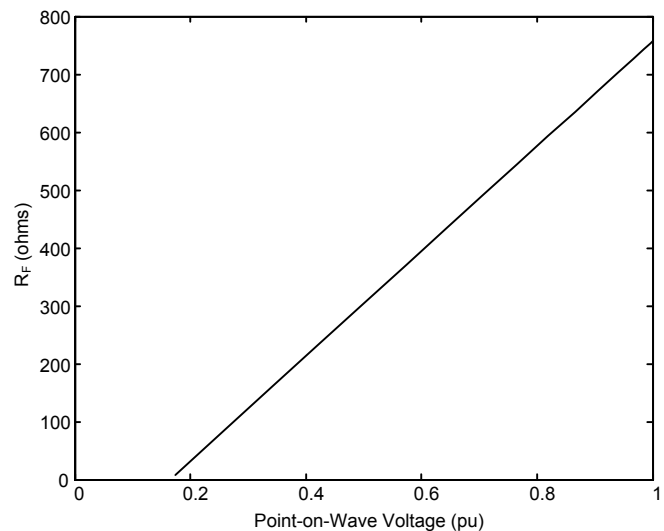


Fig. 15. Sample sensitivity plot for the TW87 element.

#### 2) Dependability and Security

Practical implementation of the TW87 element requires the operating current (the sum of the first current TWs measured at both terminals) to be greater than the restraint current (the difference of the first TW at a terminal and the TW recorded at the remote terminal after one travel time). In addition, the operating current must be greater than a threshold. Practical implementations of the TW87 element include other security conditions and therefore cause an extra loss of dependability.

Fig. 16 plots a sample dependability curve for metallic faults for the TW87 element tested for a 161 km, 500 kV line, assuming the POW distribution suggested in Section III.

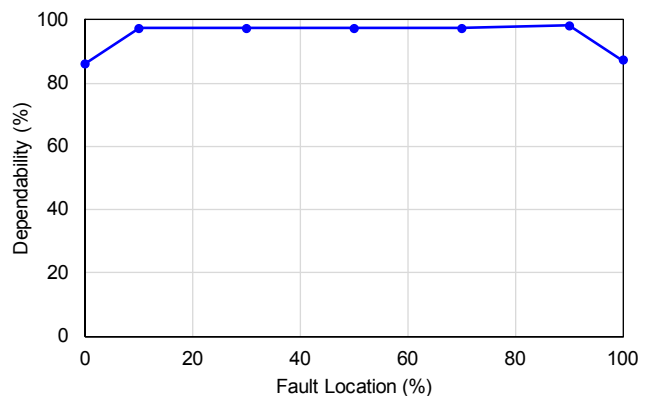


Fig. 16. Sample dependability plot for the TW87 element.

#### 3) Operating time

Unlike phasor-based or incremental quantity-based protection elements, the TW elements typically operate in a well-defined time, independent from system conditions but often dependent on the line length. In other words, we can calculate the TW87 operating time rather than test for it.

Our goal is to calculate the operating time at the local terminal for a fault at  $m$  (pu) from the local terminal. Fig. 17 shows a timing diagram of the TW87 data processing and communications.

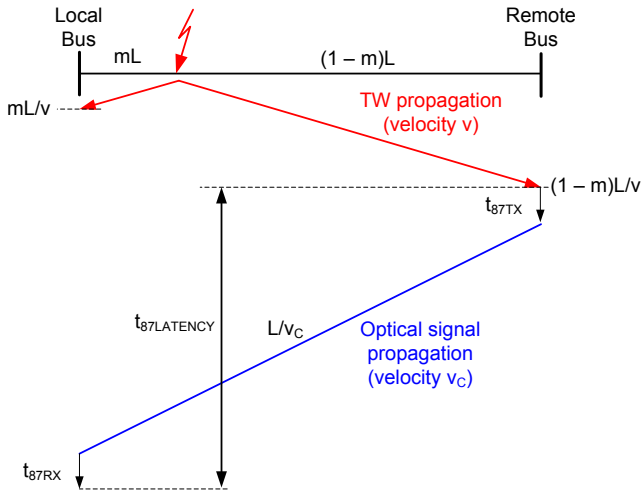


Fig. 17. Timing diagram explaining TW87 data latency.

We packetize the currents captured at the remote terminal and send them to the local terminal. There is a time penalty ( $t_{87TX}$ ) associated with this process. We assume fiber communications with the propagation velocity of  $v_C$  and the fiber length equal to the length of the protected line,  $L$ . Therefore, the data take  $L/v_C$  to travel to the local terminal. There is another time penalty associated with receiving the data at the remote terminal ( $t_{87RX}$ ). As a result, the local terminal sees the remote data with a latency of:

$$t_{87LATENCY} = \frac{L}{v_C} + t_{87TX} + t_{87RX} \quad (10)$$

As per the TW87 algorithm [2], we can finish the TW87 calculations in one line propagation time ( $T_L$ ) after we receive the very first TW at the local or remote terminal. It is important to realize that the remote data at the local terminal will always lag the local data by more than the line propagation time. Even if the fault is remote, the delay through the transmission line is shorter than the delay in the fiber ( $v > v_C$ , therefore  $L/v < L/v_C$ ). The delays associated with transmitting and receiving the data increase the difference even further.

Fig. 18 shows the time diagram for a fault at  $m$  from the local terminal. We mark four key points in the diagram:

- Time A marks when a TW from an external fault close to the local terminal would arrive at the remote terminal. We use the TW87 algorithm to check the remote data for the exiting TW. The remote data at time A are available at the local terminal after the  $t_{87LATENCY}$  time, at time A'.
- Time B marks when a TW from an external fault close to the remote terminal would arrive at the local terminal.
- Time C marks when we received the first remote TW at the local terminal with the TW originating from an internal fault at  $m$ .

Note that the first remote TW received by the local terminal will always arrive after the first local TW. Therefore, the TW87 logic will always check the local data for the exiting TW, because more local data are always available than remote data.

As a result, the local relay will finish the TW87 calculations at time A' in Fig. 18. At time A', the local data at B that are required to check for the exiting TW are guaranteed to be available.

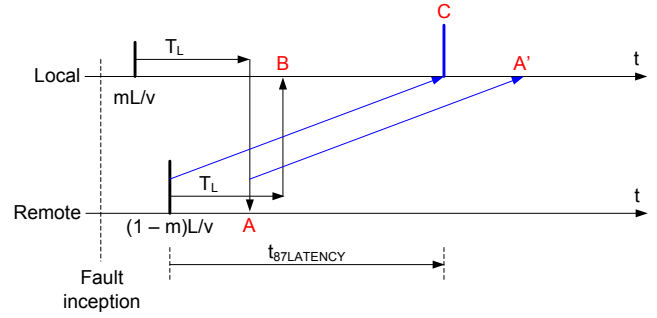


Fig. 18. Data availability in the local relay, remote data at the remote relay, and remote communications to the local relay.

The TW87 operating time measured from the fault inception is:

$$t_{87} = t_C = t_{87LATENCY} + \frac{(1-m)L}{v} \quad (11)$$

When measured from the first TW at the local terminal, the operating time is:

$$t_{87} = t_{87LATENCY} + \frac{(1-m)L}{v} - \frac{mL}{v} \quad (12)$$

We require one additional processing interval to pass the TW87 outputs to the trip logic of the relay. We use (10) for the latency, simplify (12), and obtain the following TW87 operating time:

$$t_{87} = L \left( \frac{1-2m}{v} + \frac{1}{v_C} \right) + t_{87TX} + t_{87RX} + t_{PROC} \quad (13)$$

Looking closely at (13), we notice that the operating time for remote faults is shorter than for close-in faults:

$$m = 0 \rightarrow t_{87} = L \left( \frac{1}{v_C} + \frac{1}{v} \right) + t_{87TX} + t_{87RX} + t_{PROC} \quad (14)$$

$$m = 1 \rightarrow t_{87} = L \left( \frac{1}{v_C} - \frac{1}{v} \right) + t_{87TX} + t_{87RX} + t_{PROC} \quad (15)$$

We need to keep in mind that in (13), we measure the operating time from the first TW at the local terminal. If we measure the operating time from the fault inception, we obtain:

$$t_{87} = L \left( \frac{1-m}{v} + \frac{1}{v_C} \right) + t_{87TX} + t_{87RX} + t_{PROC} \quad (16)$$

The time calculated in (16) also depends on the fault location. Notice that the relay that is farthest from the fault location operates the fastest.

A slightly different implementation of the TW87 element compares both pairs of the first and exiting TWs: first local TW with the exiting remote TW, and first remote TW with the exiting local TW. Using this logic, the relay needs to wait longer for the available data. If we repeat our calculations for this TW87 logic, we will obtain an operating time as follows:

$$t_{87} = L \left( \frac{1}{v} + \frac{1}{v_C} \right) + t_{87TX} + t_{87RX} + t_{PROC} \quad (17)$$

One particular implementation has the transmit and receive delays of 0.05 ms and the processing interval of 0.1 ms. For a 300 km line, this implementation will operate as follows:

$$300 \cdot \left( \frac{1}{300 \cdot 10^3} + \frac{1}{1.6 \cdot 300 \cdot 10^3} \right) + 0.05 \cdot 10^{-3} + 0.05 \cdot 10^{-3} + 0.1 \cdot 10^{-3} = 3.63 \text{ ms}$$

This time is constant and independent from system conditions or the fault location.

## VI. FAULT-INDUCED TWS VS HIGH-FREQUENCY INTERFERENCE

As shown in the previous sections, UHS line protective relays make extensive use of the information contained in the high-frequency transients. With input signal bandwidth potentially exceeding 500 kHz, it is prudent to ask how UHS relays behave when subject to type-test signals where the energy falls within the measurement range of the relay. This situation is very different from phasor-based relays that use extensive front-end filtering in hardware and software to remove and smooth out the type-test transients. The very fast response of UHS relays further complicates type testing.

Table I shows approximate bandwidth associated with typical type-test signals.

TABLE I  
TYPE TEST SIGNAL BANDWIDTH

Test Name	Signal Shape	Signal Bandwidth
Lightning Surge	1.2/50 $\mu$ s pulse	0.02 to 1 MHz
Fast Transient Burst	5/50 ns, 5 to 100 kHz repetition	0.005 to 200 MHz
1 MHz Damped Oscillatory	1 MHz with 75 ns/10 $\mu$ s envelope	0.1 to 10 MHz

While it is clear that UHS relays must be able to operate in the substation environment, and must therefore be able to pass prescribed type tests, it is important to put these requirements in context and take a more detailed look at the history of these tests and the way the industry originally defined them. It is also important to take a more detailed look at a common misconception that standardized type-test waveforms fully represent actual power system events and the substation environment.

We start by noting that type-test waveforms, originally defined in the IEEE C37.90 [11] standard series and more recently consolidated in IEEE 1613 [12] and IEC 60255-26 [13], represent the worst-case misoperation event knowledge collected over the hundred-year history of our industry.

Knowledge accumulation started with electromechanical relays, whose inertia and energy required to perform mechanical action prevented the relays from misoperations on high-frequency transients. Early type tests, therefore, do not focus on misoperations but on insulation coordination and the ability of the relay to survive switching overvoltage. Simple impulse voltage tests with no energizing quantities, such as IEEE C37.90, were sufficient for this purpose.

The industry discovered new susceptibilities when the protective relays started using solid-state, and later, microprocessor-based technologies. Practitioners noticed that some of the new devices were susceptible to hand-held radio transceivers, electrostatic discharge, fast-switching transients caused by auxiliary relays and disconnect switches, etc. This knowledge resulted in creation of the radiated and conducted radio frequency (RF) immunity, fast transient, electrostatic discharge, and other C37.90 series tests.

Similar to an astronaut training program in which the young candidate is exposed to all known types of stress, it is well understood that no individual test fully emulates the actual mission environment. In effect, type tests can be seen as nothing more than a series of well-defined, repeatable obstacles whose breadth and variety collectively ensure that the relay does not contain an obvious design weakness.

It is also important to note that because of being collected over many years and based on field experience, standardized type tests are inherently targeted at legacy technologies. This means that there is no good reference showing how such transients should be applied to the UHS relays and how UHS relays should respond to them.

An interesting property of the latest UHS relays is their ability to faithfully record the high-frequency disturbances present at their input terminals including the type-test transients. For the first time in history, practicing engineers will be able to see and measure—at scale—the actual interference present in their substations. Some of this interference may make it impossible to perform some intended UHS relay functions in a particular location, but that may be acceptable as long as the relay remains secure and capable of alerting the user to the situation. High-precision event records will be crucial in addressing this industry challenge.

Below we share some early results obtained while testing a UHS relay. We concentrate on a single test: the lightning surge transient defined in IEC 60255-26. This test is simple, yet sufficient to illustrate the broader test challenge.

IEC 60255-26 prescribes that the relay be exposed to a 2 kV, 1.2 by 50  $\mu$ s lightning surge waveform applied differentially across the voltage and current inputs. Since current inputs present an effective short circuit at the frequencies of interest, a surge test generator will inject a current pulse whose magnitude is determined by the specified generator source impedance (42  $\Omega$ ). The current entering the UHS relay terminals will be in the order of  $2 \text{ kV}/42 \Omega = 47.6 \text{ A}$ , which fits well within the measurement range of the 5 A nominal current inputs. Fig. 19 shows a surge waveform recorded during this test.

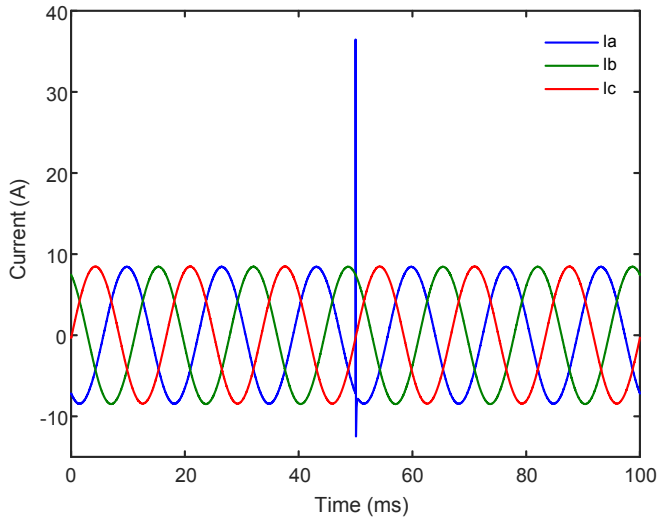


Fig. 19. Lightning surge waveform recorded by the UHS relay current input.

Fig. 20 shows the same surge waveform on a microsecond scale.

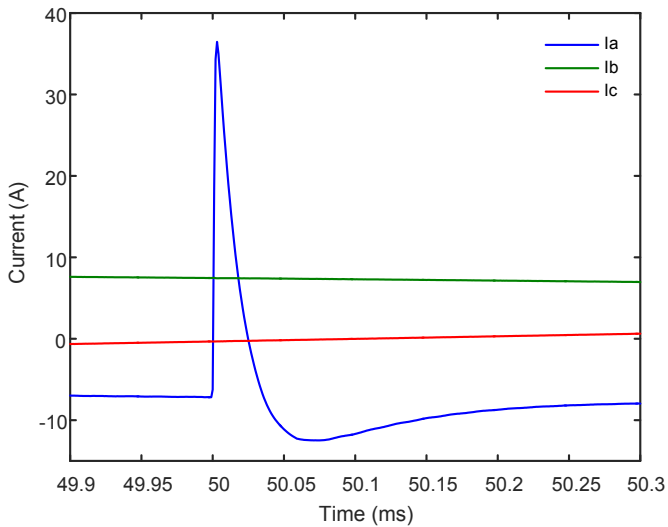


Fig. 20. Current surge waveform detail (2 kV, 1.2/50  $\mu$ s transient applied differentially through a 42  $\Omega$  coupling network impedance).

The waveform of Fig. 20 is very clean and faithfully reproduced by the high-fidelity UHS relay measurement circuitry. Neighboring channel crosstalk is exceptionally low and buried in noise. It is important to note that we achieved the reported result by carefully arranging the decoupling network inductors, which were the limiting factor for cross channel coupling. We had to space apart individual inductors and rotate them 90 degrees with respect to each other, as shown in Fig. 21. This required test arrangement, points to the fact that UHS relay testing calls for a cleaner and better controlled test setup. The experience our industry gains from testing UHS relays can lead to further refinement of applicable type-test standards.

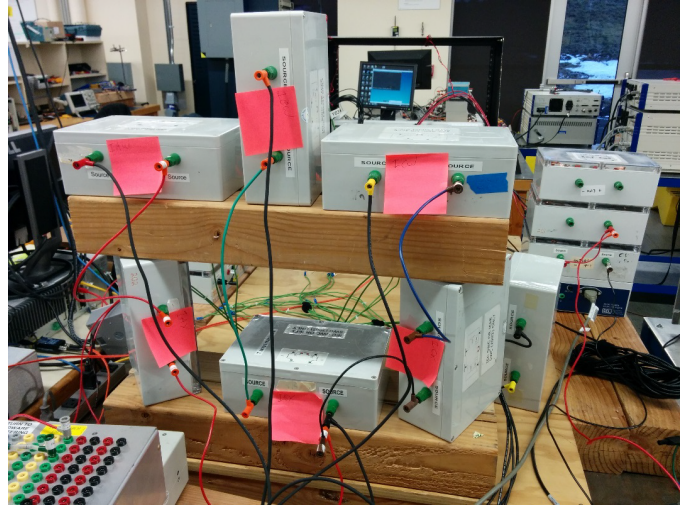


Fig. 21. Decoupling network setup optimized for lowest crosstalk between channels.

The differential surge test is much more difficult for the UHS relay voltage channel. An input rated for 115 Vac (66.4 V line-to-neutral) may for example be designed to clip at  $\pm 280$  V peak. The question then becomes, what should this input do when faced with the 2 kV surge waveform?

Fig. 22 shows the A-phase voltage of a particular UHS relay, captured during the 2 kV surge test on the Va channel. Voltage waveforms are clean with very small crosstalk transients detected on the B and C phases. Waveform detail in Fig. 23 shows clean clipping at 287 V with instantaneous recovery from the overvoltage/clipping state, allowing the relay to faithfully follow the input waveform as soon as its voltage comes within the specified operating range of the analog-to-digital converter.

Behavior in Fig. 23 is the best expected performance of any device in this situation. However, this means that the UHS relay algorithm must be able to reliably recognize the surge test condition and block the voltage-based elements until the inputs return within specified limits.

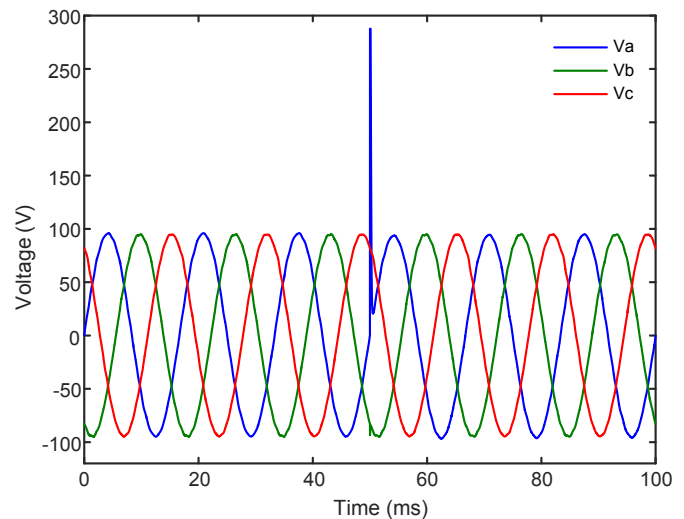


Fig. 22. Lightning surge waveform recorded by the UHS relay voltage input.

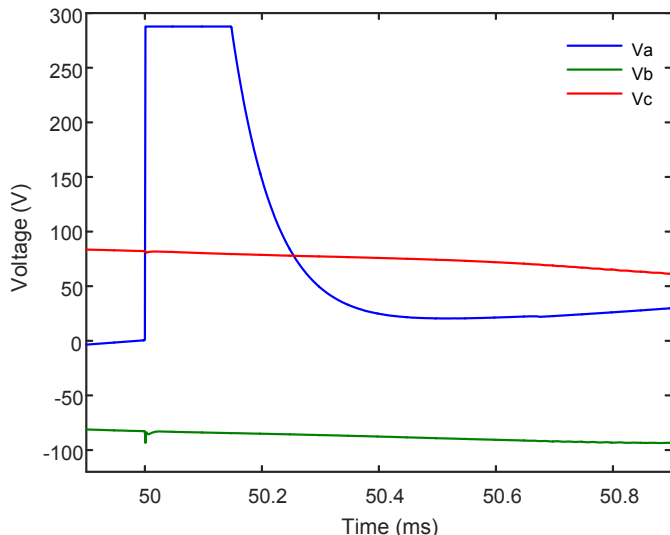


Fig. 23. Voltage surge waveform detail (2 kV, 1.2/50  $\mu$ s waveform applied differentially to the voltage input).

Temporarily disabling the protection element is acceptable for a rare lightning strike event in the immediate vicinity of the relay. But what should the relay do if the blocking occurs more often? Our answer to that question is to design the UHS relay with advanced type-test diagnostics and logging and alarming capabilities, thus providing the user with full confidence about both the device operation and the associated substation environment. High bandwidth recording capability is a unique UHS relay feature that enables utility engineers and relay designers to fully understand the electromagnetic compatibility (EMC) environment in which their relays are called to operate.

Industry knowledge of the typical substation high-frequency EMC environment is still very limited. For example, data we collected using the first TW fault-locating relay show that the current measurements are clean. Over hundreds of locations, we observed no fast transient, 1 MHz oscillatory or unintended lightning surge waveform signatures. At the same time, the relay TW subsystem sensitivity in question is so high, one of the relays was able to record TW reflections traveling a distance in excess of 800 km. These results do not eliminate or invalidate the need for applying type-test transients to the relays, but do shine a new light on these tests as alternate means of subjecting the relays to high levels of conducted and radiated disturbances. The type-test waveforms provided by today's standards may not be real, but they still do a great job of hardening our designs and contributing to the security of our protection schemes.

Going forward, the authors expect the UHS relays to serve as a catalyst, putting additional demands on test laboratories. UHS relays will be able to expose various test setup issues, driving the laboratories to further update their test methods and equipment.

Standards writing bodies will likely need to update some of the test requirements, making the tests more specific and more repeatable in the process. Coupling and decoupling networks may need to be further refined based on UHS relay recordings (actual waveforms applied to the device under test were mostly inaccessible in the past). The existing spirit of the type test, however, is likely to persist, with modifications applying

primarily to the application devices and methods. The authors are looking forward to applying the practical knowledge gained over the next few years to improve the quality of international standards and our understanding of the substation EMC environment.

## VII. TRANSIENT SIMULATION TOOLS

Transient simulation tools aid in evaluating the performance of protective relays. This is especially true for UHS relays that use the high-frequency components of their input voltages and currents, including TWs. These relays sample and process their input voltage and current signals at 1 MHz or higher. In order to test TW-based protection elements, we require simulation tools to model voltage and current signals that include the TW information at rates of at least twice the sampling frequency. The changes that occur within several hundred microseconds up to about a millisecond after the fault, contain information that the TW-based UHS relays use in their protection algorithms.

### A. Transient Modeling Considerations

#### 1) Transmission Lines

Transient simulation programs must take into account the changes in conductor resistance and inductance due to skin effect for proper transmission line modeling [14] [15]. Fig. 24 shows how the current waves propagate across a 400 kV line in response to nominal voltage steps applied on the A-phase and B-phase at the sending end (the step change occurs at  $t = 0$ ). In this case, the impedance termination matches the characteristic impedance of the line, thereby eliminating wave reflections. Notice the dispersion of the current signals (rounding of the wave front) as they travel along the line.

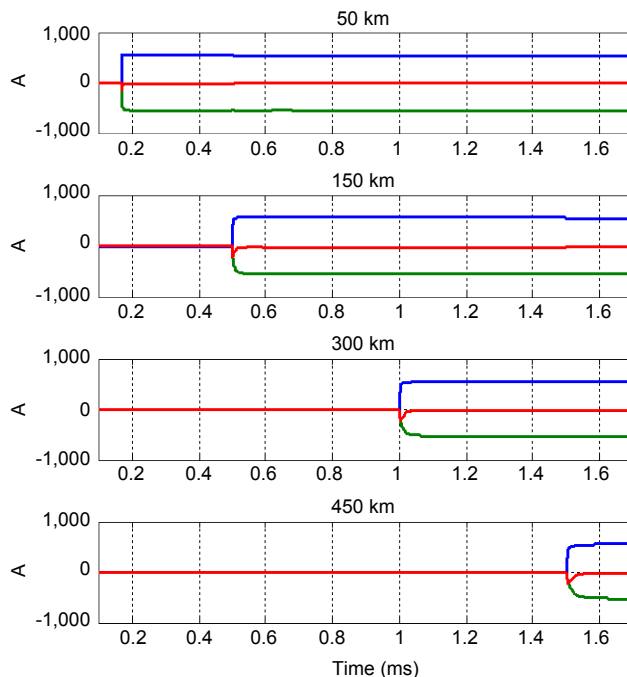


Fig. 24. Current waves at 50, 150, 300, and 450 km traveling on a 400 kV line for voltage step changes at the sending end, where A-phase is green, B-phase is blue, and C-phase is red.

Line modeling should include ground wires. Ground wires are routinely accounted for by the simulation programs, but the wires are buried in the equivalent matrices. Therefore, the ground wire terminals are not accessible for simulating events such as lightning strikes. It is possible to simulate the ground wires as a parallel transmission line with adequate conductor positions and grounding to simulate the tower footing resistance.

2) Current Transformers

UHS relays obtain their voltage and current signals from conventional instrument transformers. Therefore, CT models should, in addition to the saturation characteristic, take into account stray capacitance effects at high frequencies. Fig. 25 shows the equivalent electric circuit for an iron-core CT while Fig. 26 shows the inverse of the ratio correction factor (RCF) as a function of frequency of a typical iron-core CT [16]. A large core cross-sectional area and low leakage inductances are desirable CT characteristics for achieving improved bandwidth. Window-type CTs have adequate bandwidth (with cutoff frequencies in the hundreds of kilohertz) and provide adequate TW information for the correct operation of a UHS relay.

Long secondary cabling can cause ringing in the secondary wires—current TWs reflected back and forth between the CT secondary winding terminals and the relay terminals. A 300 m cable run may have a propagation time in the order of 1–2  $\mu$ s. When modeling cable runs as distributed circuits with TWs, we may need to shorten the simulation step to a small fraction of a microsecond.

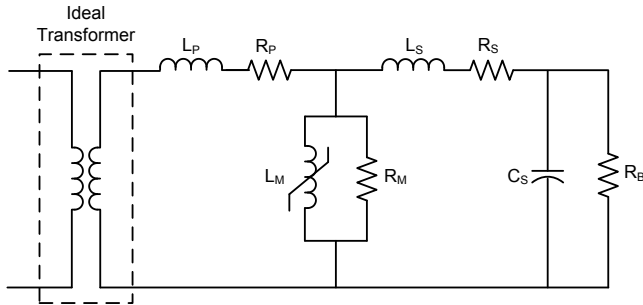


Fig. 25. CT equivalent electric circuit model including stray capacitances for modeling transients.

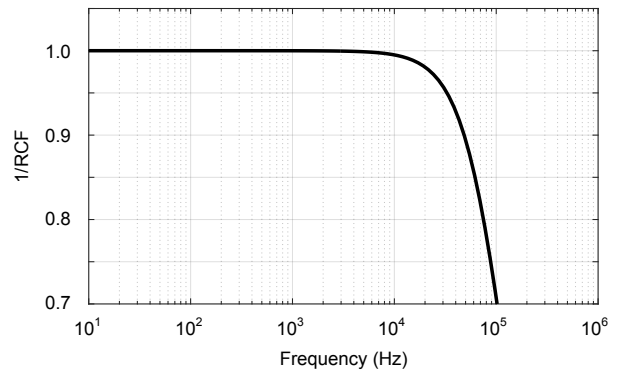


Fig. 26. Inverse of the ratio correction factor of a typical iron-core CT as a function of frequency.

3) CCVTs

CCVT models should also consider the stray capacitance ( $C_c$ ) of the tuning reactor, the stray capacitances of the primary and secondary windings ( $C_p$  and  $C_s$ ) of the step-down transformer (SDT), and the stray interwinding capacitance ( $C_{ps}$ ) across the SDT. Fig. 27 shows the electrical equivalent circuit of a CCVT with a ferroresonance suppression circuit (FSC) suitable for modeling voltage transients. Fig. 28 shows the magnitude frequency response of a typical CCVT with FSC (validated with field tests) for up to 10 kHz [17]. The CCVT has reduced bandwidth compared to the CT bandwidth.

CCVT response above 10 kHz depends strongly on the device design, and although incidental (driven by stray capacitances), it should be reasonably repeatable for a particular CCVT design or type. Literature documenting this is not readily available.

In addition, one must pay attention to the location of CTs, CCVTs, line traps, etc. and consider the actual location of the physical equipment. For example, when simulating line traps, one should place the CCVT on the line side reflecting the physical location of the CCVT. With CCVTs placed on the bus, the line trap impact will not be correctly represented because the circuit would lack a low-impedance path at high frequencies (a CCVT) at the line side of the line trap.

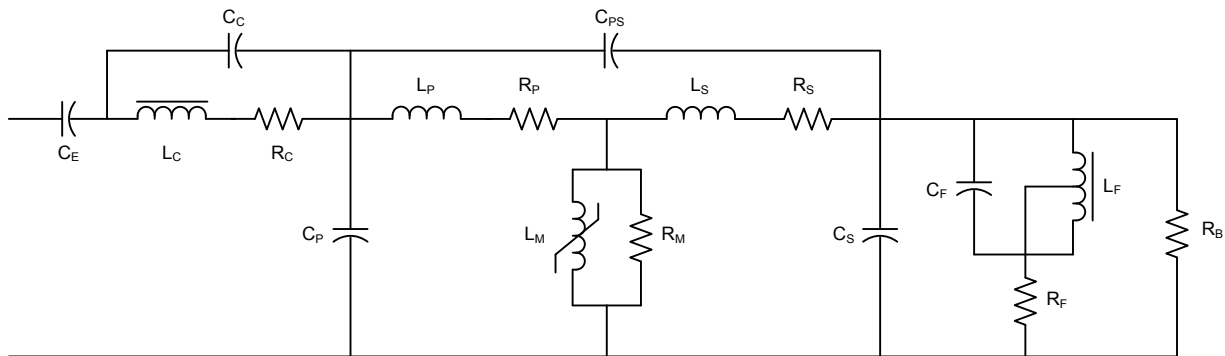


Fig. 27. CCVT equivalent electric circuit model including stray capacitances, ferroresonance suppression circuit, and burden resistor.

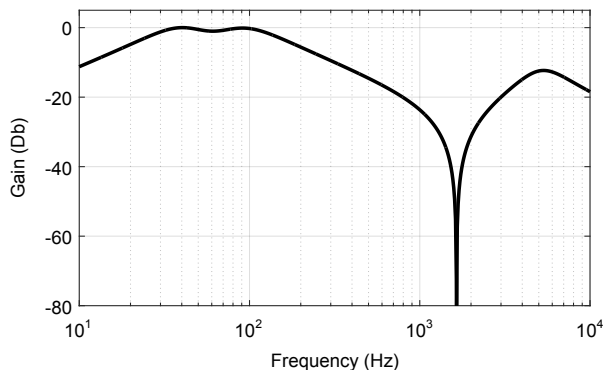


Fig. 28. Magnitude frequency response of a typical CCVT with a ferroresonance suppression circuit.

#### 4) Line Termination

When considering voltages and currents in the TW spectrum of hundreds of kilohertz, various elements come into play that are normally neglected when simulating the network for the system frequency and up to a few kilohertz. Following are examples of power system elements that we should consider in simulation tools to properly represent TW phenomena for TW relay testing:

- Bus capacitance. It impacts the TW termination effect.
- Any shunt power capacitors on the bus. They dramatically impact the TW termination effect.
- Line traps. They impact the TW termination effect and may cause ringing in the TWs at carrier frequencies.
- Surge arresters. They may conduct during lightning strikes drawing current inside the line protection zone.
- Shunt reactors including stray winding capacitances.
- CCVTs. They create a low-impedance path and change the TW termination effects.

#### B. Relay Modeling and Relay Testing

We use accurate computer models of the protection algorithms for verifying their performance using signals from EMTF power system models. After numerical relays convert the voltage and current measurements to digital signals, numerical relay algorithms and their corresponding computer models can have virtually identical responses. Furthermore, relays with playback capability can feed digitized voltage and current signals from transient simulations or from events captured during actual power system faults or disturbances to the protection algorithms of the relay for post-fault analysis, as Fig. 29 illustrates. Normally, we expect the actual events to be captured with the same relay hardware as the relay under test.

The main challenge when testing UHS relays is to apply secondary voltage and current signals that are accurate in the frequency spectrum from a few hertz to a few hundred kilohertz. Traditional test equipment tests relays that sample voltages and currents at or below 8 kHz; these relays are usually phasor-based and process protection algorithms at rates not greater than 2 kHz.

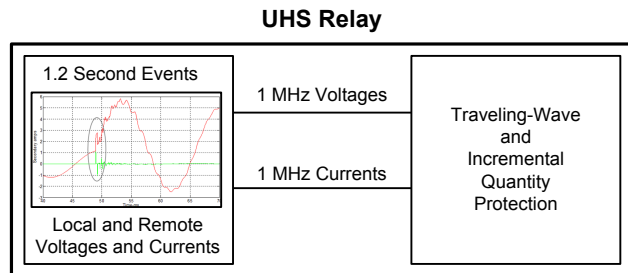


Fig. 29. UHS relay with event playback capability can replicate protection element operation for post-fault analysis.

Typically, real-time digital simulators [18] model the power system at time intervals of approximately  $42 \mu\text{s}$  (for simulations running at 24 kHz). Additionally, power amplifiers limit the test signal bandwidth to 25 kHz or less. Real-time digital simulators are sufficient to test incremental quantity-based elements. However, today, they are not adequate for testing TW protection elements. To overcome these limitations, we tested the UHS relays as follows:

#### 1) Signal Injection With a Traveling-Wave Source

The test system in Fig. 30 includes a traveling-wave source (TWS) that generates TW current step signals with microsecond rise times for two relays under test; the current outputs generate 5 A pulses. We can shift the TW transients in time to emulate faults at different locations along the line with nanosecond-level accuracy. We used this system to test the accuracy of a TW fault locator in a line current differential (87L) relay [10].

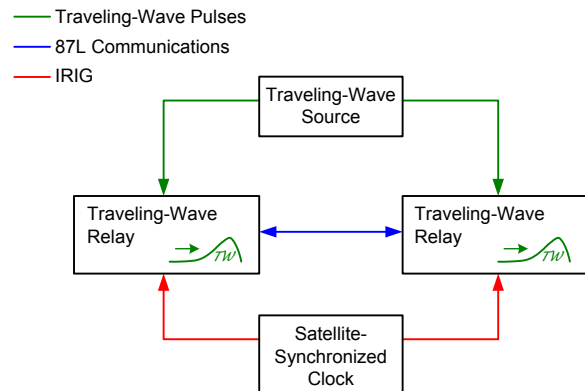


Fig. 30. Testing TW fault locators using a TWS.

#### 2) Signal Injection With a Traveling-Wave System

To test, UHS TW-based relays, we can combine the signals from the TWS with signals from a traditional test system. The combined signals include the operating system frequency component and TW component, as Fig. 31 illustrates. This testing approach emulates faults that are close to the actual power system faults and allows us to test UHS relays that respond to TWs. Coupling filters are very important in this test setup in order to ensure that the TW signals from the TWS are directed toward the relay and not toward the traditional test set, potentially damaging the latter.

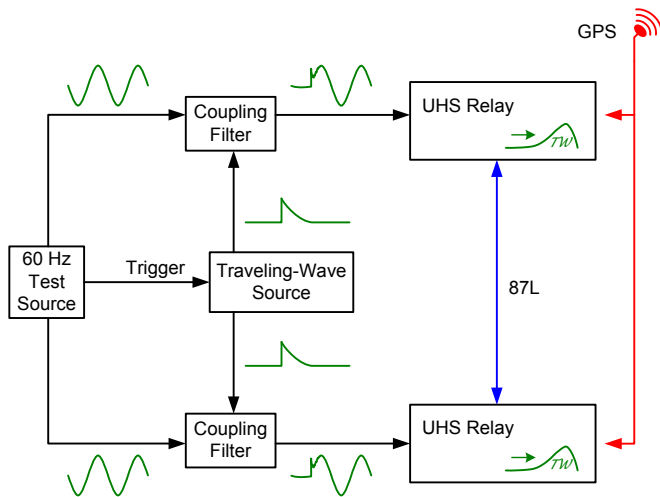


Fig. 31. Testing UHS relays using a system that combines signals from a TWS and a system frequency source.

### VIII. CONCLUSIONS

High-performance UHS relays use subtle signal features in their input currents and voltages that call for more attention when testing these relays. While commissioning testing is relatively easy, primarily because the relays use only a few simple settings, certification and type testing requires wide-bandwidth signal sources and test signals that produce realistic power system events.

Incremental quantity-based protection elements require realistic test signals up to a frequency of about 1 kHz. EMTP-generated signals are best for performance testing, either in an open-loop playback or using closed-loop simulators, such as real-time digital simulators. We can use traditional test sets to commission-test these elements by injecting power system frequency voltages and currents. These signals must be coherent with the applied settings in terms of the line impedances, system impedance, X/R ratio, etc. When generating test signals, it is preferable to model transitions from prefault to fault conditions, including the decaying dc offset for the currents. Today's test sets are well suited for testing incremental quantity-based protection elements.

TW-based protection elements require realistic test signals up to a frequency of about 500 kHz. Presently, no closed-loop real-time digital simulators are widely available that can test TW-based elements. Instead, we can perform an open-loop test using equipment with a high-bandwidth playback. Apply submicrosecond simulation time steps and frequency-dependent transmission line models when using EMTP for testing the performance of TW-based protection elements. To commission-test the TW-based elements, we can use step signals, superimposed on the power system components. Today's test sets are not capable of generating step changes that have an adequate rise time and a precise enough timing control. New TW-capable test sets are emerging, however, allowing simple and accurate methods of testing TW protection and fault locators. These new test sets can operate in conjunction with traditional test sets.

UHS relays perform far better in terms of speed and sensitivity than phasor-based relays. This dramatically higher level of performance calls for precise and methodical definitions of performance measures when specifying, testing, and comparing these relays. In this paper, we proposed a number of formal performance measures suitable for documenting the performance of any given relay as well as for providing an informed comparison between multiple relays. UHS relays are biased for speed not dependability. Therefore, one of the performance measures we advocate is dependability. We defined dependability numerically and showed how to plot it when evaluating relays.

UHS relays, especially the relays with TW-based elements, are so fast that their operating times approach the communications channel latencies even when using direct fiber. Therefore, a precise measure of the protection scheme operating time should include the channel delay. The total time may depend on the fault location, as it takes some time for the TW to reach the line terminals. This impact of TW propagation time is already in effect for phasor-based relays, but it is not clearly visible because the speed of phasor-based protection elements is much slower than the speed of TW-based elements.

Finally, TW-based relays will give our industry an opportunity to gain detailed knowledge about the substation environment and refine our EMC type-test setups and requirements. The installed base of these relays will generate a large volume of evidence of the high-frequency signals present at the relay terminals. Such data will allow us to define more realistic type-tests and further improve our practices for the benefit of future power systems.

### IX. ACKNOWLEDGEMENT

The authors would like to acknowledge the contributions of SEL hardware engineers Tracey Windley and Zack Sheffield to sections on type testing and relay testing with traveling waves.

### X. REFERENCES

- [1] E. O. Schweitzer, III, B. Kasztenny, A. Guzmán, V. Skendzic, and M. V. Mynam, "Speed of Line Protection – Can We Break Free of Phasor Limitations?" proceedings of the 41st Annual Western Protective Relay Conference, Spokane, WA, October 2014.
- [2] E. O. Schweitzer, III, B. Kasztenny, and M. V. Mynam, "Performance of Time-Domain Line Protection Elements on Real-World Faults," proceedings of the 42nd Annual Western Protective Relay Conference, Spokane, WA, October 2015.
- [3] G. Benmouyal and J. Roberts, "Superimposed Quantities: Their True Nature and Application in Relays," proceedings of the 26th Annual Western Protective Relay Conference, Spokane, WA, October 1999.
- [4] K. Lee, D. Finney, N. Fischer, and B. Kasztenny, "Testing Considerations for Line Current Differential Schemes," proceedings of the 37th Annual Western Protective Relay Conference, Spokane, WA, October 2010.
- [5] D. P. Kothari and I. J. Nagrath, *Modern Power System Analysis*, McGraw-Hill, 2006, pp. 369.
- [6] IEEE Power System Relaying Committee Report, "Single Phase Tripping and Auto Reclosing of Transmission Lines," IEEE Transactions on Power Delivery, Vol. 7, Issue 1, January 1992, pp. 182–192.
- [7] H. Altuve, K. Zimmerman, and D. Tziouvaras, "Maximizing Line Protection Reliability, Speed, and Security," proceedings of the 42nd Annual Western Protective Relay Conference, Spokane, WA, October 2015.

- [8] E. O. Schweitzer, III, N. Fischer, and B. Kasztenny, "A Fresh Look at Limits to the Sensitivity of Line Protection," proceedings of the 38th Annual Western Protective Relay Conference, Spokane, WA, October 2011.
- [9] H. W. Dommel, *Electromagnetic Transients Program: Reference Manual: (EMTP Theory Book)*. Bonneville Power Administration, August 1986.
- [10] E. O. Schweitzer, III, A. Guzmán, M. V. Mynam, V. Skendzic, B. Kasztenny, and S. Marx, "Locating Faults by the Traveling Waves They Launch," proceedings of the 40th Annual Western Protective Relay Conference, Spokane, WA, October 2013.
- [11] IEEE Standard C37.90-2005, IEEE Standard for Relays and Relay Systems Associated With Electric Power Apparatus.
- [12] IEEE Standard 1613-2009, IEEE Standard Environmental and Testing Requirements for Communications Networking Devices in Electric Power Substations.
- [13] IEC 60255-26:2013, Measuring Relays and Protection Equipment – Part 26: Electromagnetic Compatibility Requirements.
- [14] J. R. Martí, "Accurate Modelling of Frequency Dependent Transmission Lines in Electromagnetic Transient Simulations," *IEEE Transactions on Power Applications and Systems*, Vol. PAS-101, Issue 1, January 1982, pp. 147–155.
- [15] P. Moreno, P. Gómez, J. L. Naredo, and J. L. Guardado, "Frequency Domain Transient Analysis of Electrical Networks Including Non-linear Conditions," *International Journal of Electrical Power & Energy Systems*, Vol. 27, Issue 2, February 2005, pp. 139–146.
- [16] R. C. Dugan, M. F. McGranaghan, and H. W. Beaty, *Electric Power Systems Quality*. McGraw Hill, New York, 1996, ISBN 0-07-018031-8.
- [17] M. Kezunovic, L. Kojovic, V. Skendzic, C. W. Fromen, D. Sevcik, and S. L. Nilsson, "Digital Models of Coupling Capacitor Voltage Transformers for Protective Relay Studies," *IEEE Transactions on Power Delivery*, Vol. 7, Issue 4, October 1992, pp. 1927–1935.
- [18] R. Kuffel, J. Giesbrecht, T. Maguire, R. P. Wierckx, and P. McLaren, "RTDS – A Fully Digital Power System Simulator Operating in Real Time," proceedings of the ICDS-95, College Station, Texas, USA, April 1995, pp. 19–24.

## XI. BIOGRAPHIES

**Dr. Edmund O. Schweitzer, III** is recognized as a pioneer in digital protection and holds the grade of Fellow in the IEEE, a title bestowed on less than one percent of IEEE members. In 2002, he was elected as a member of the National Academy of Engineering. Dr. Schweitzer received the 2012 Medal in Power Engineering, the highest award given by IEEE, for his leadership in revolutionizing the performance of electrical power systems with computer-based protection and control equipment. Dr. Schweitzer is the recipient of the Regents' Distinguished Alumnus Award and Graduate Alumni Achievement Award from Washington State University and the Purdue University Outstanding Electrical and Computer Engineer Award. He has also been awarded honorary doctorates from both the Universidad Autónoma de Nuevo León, in Monterrey, Mexico, and the Universidad Autónoma de San Luis Potosí, in San Luis Potosí, Mexico, for his contributions to the development of electric power systems worldwide. He has written dozens of technical papers in the areas of digital relay design and reliability, and holds over 180 patents worldwide pertaining to electric power system protection, metering, monitoring, and control. Dr. Schweitzer received his bachelor's and master's degrees in electrical engineering from Purdue University, and his doctorate from Washington State University. He served on the electrical engineering faculties of Ohio University and Washington State University, and in 1982, he founded Schweitzer Engineering Laboratories, Inc. to develop and manufacture digital protective relays and related products and services.

**Bogdan Kasztenny** is the R&D director of protection technology at Schweitzer Engineering Laboratories, Inc. He has over 25 years of expertise in power system protection and control, including 10 years of academic career and 15 years of industrial experience, developing, promoting, and supporting many protection and control products. Bogdan is an IEEE Fellow, Senior Fulbright Fellow, Canadian representative of CIGRE Study Committee B5, registered professional engineer in the province of Ontario, and an adjunct professor at the University of Western Ontario. Bogdan serves on the Western Protective Relay Conference Program Committee (since 2011) and on the Developments in

Power System Protection Conference Program Committee (since 2015). Bogdan has authored about 200 technical papers and holds 30 patents.

**Mangapathirao (Venkat) Mynam** received his MSEE from the University of Idaho in 2003 and his BE in electrical and electronics engineering from Andhra University College of Engineering, India, in 2000. He joined Schweitzer Engineering Laboratories, Inc. (SEL) in 2003 as an associate protection engineer in the engineering services division. He is presently working as a senior research engineer in SEL research and development. He was selected to participate in the U. S. National Academy of Engineering (NAE) 15th Annual U. S. Frontiers of Engineering Symposium. He is a senior member of IEEE and holds eight patents in the areas of power system protection, control, and fault location.

**Armando Guzmán** received his BSEE with honors from Guadalajara Autonomous University (UAG), Mexico. He received a diploma in fiber-optics engineering from Monterrey Institute of Technology and Advanced Studies (ITESM), Mexico, and his masters of science and PhD in electrical engineering and masters in computer engineering from the University of Idaho, USA. He served as regional supervisor of the Protection Department in the Western Transmission Region of the Federal Electricity Commission (the electrical utility company of Mexico) in Guadalajara, Mexico for 13 years. He lectured at UAG and the University of Idaho in power system protection and power system stability. Since 1993 he has been with Schweitzer Engineering Laboratories, Inc. in Pullman, Washington, where he is a fellow research engineer. He holds numerous patents in power system protection and metering. He is a senior member of IEEE.

**Normann Fischer** received a Higher Diploma in Technology, with honors, from Technikon Witwatersrand, Johannesburg, South Africa, in 1988; a BSEE, with honors, from the University of Cape Town in 1993; an MSEE from the University of Idaho in 2005; and a PhD from the University of Idaho in 2014. He joined Eskom as a protection technician in 1984 and was a senior design engineer in the Eskom protection design department for three years. He then joined IST Energy as a senior design engineer in 1996. In 1999, Normann joined Schweitzer Engineering Laboratories, Inc., where he is currently a fellow engineer in the research and development division. He was a registered professional engineer in South Africa and a member of the South African Institute of Electrical Engineers. He is currently a senior member of IEEE and a member of the American Society for Engineering Education (ASEE).

**Veselin Skendzic** is a principal research engineer at Schweitzer Engineering Laboratories, Inc. He earned his BS in electrical engineering from FESB, University of Split, Croatia; his Masters of Science from ETF, Zagreb, Croatia; and his PhD from Texas A&M University, College Station, Texas. He has more than 25 years of experience in electronic circuit design and power system protection-related problems. He is a senior member of IEEE, has written multiple technical papers, has over 20 patents, and is actively contributing to IEEE and IEC standard development. He is a member of the IEEE Power Engineering Society (PES) and the IEEE Power System Relaying Committee (PSRC) and a past chair of the PSRC Relay Communications Subcommittee (H).